






hashin_shtrikman_mp: a package for the optimal design and discovery of multi-phase composite materials

Carla J. Becker¹, Hrushikesh Sahasrabudhe^{2,3}, Max C. Gallant^{2,4},
Anubhav Jain³, Kristin A. Persson^{2,4}, and Tarek I. Zohdi¹

¹ Department of Mechanical Engineering, University of California, Berkeley, California, United States of America  ² Department of Materials Science and Engineering, University of California, Berkeley, California, United States of America ³ Energy Technologies Area, Lawrence Berkeley National Laboratory, Berkeley, CA 94720, USA ⁴ Materials Sciences Division, Lawrence Berkeley National Laboratory, Berkeley, California, United States of America  Corresponding author

DOI: [10.xxxxxx/draft](https://doi.org/10.xxxxxx/draft)

Software

- [Review](#) 
- [Repository](#) 
- [Archive](#) 

Editor: [Open Journals](#) 

Reviewers:

- [@openjournals](#)

Submitted: 01 January 1970

Published: unpublished

License

Authors of papers retain copyright and release the work under a

Creative Commons Attribution 4.0 International License ([CC BY 4.0](#))

Summary

hashin_shtrikman_mp is a tool for composites designers who have desired composite properties in mind, but who do not yet have an underlying formulation. The library utilizes the tightest theoretical bounds on the effective properties of composite materials with unspecified microstructure – the Hashin-Shtrikman bounds – to identify candidate theoretical materials, find real materials that are close to the candidates, and determine the optimal volume fractions for each of the constituents in the resulting composite. Its i) leveraging of materials in the [Materials Project](#) database, ii) integration with the [Materials Project API](#), iii) use of genetic machine-learning and iv) agnosticism to underlying microstructure, and v) ultimate engineering application, make it a tool with much broader applications than its predecessors.

Statement of need

Composites are ubiquitous in engineering due to their tunability and enhanced material properties as compared to their individual constituents. As such, composite design is an active field, but the pursuit of new materials through experimentation is expensive. Today, computational tools for materials design are integral to reducing the cost and increasing the pace of innovation in sectors like energy, electronics, aviation and beyond.

Several Python packages already exist for specific areas in composites modeling, such as [CompositesLib](#), [Compysite](#), [FeCLAP](#), and [material-mechanics](#), all of which perform stress analysis on laminates and/or fiber-reinforced composites using either classical laminate theory or the finite element method. Others exist which, like hashin_shtrikman_mp, utilize the Hashin-Shtrikman bounds on effective composite properties, such as [BurnMan](#) for thermal analysis of composite rocks/assemblages, [rockphypy](#) for mechanical modeling of sand-shale systems, ([Zare & Rhee, 2017](#))'s modeling of clay nanocomposites, and ([Zerhouni et al., 2019](#))'s modeling of 3D printed microstructures. All of these tools, however, are highly specific to composite microstructure, macro-geometry, and composition. More notably, they focus on analysis of already well-defined composites, rather than discovery of new materials.

hashin_shtrikman_mp is intended for composites designers who are much earlier in their design process – designers who are seeking out new composite formulations and who are not yet tied to a specific underlying microstructure. hashin_shtrikman_mp defines an inverse problem wherein composite formulations which achieve a desired behavior are found by minimizing a

cost function (Zohdi, 2012). Accounting for both absolute error from the desired properties and targeting even load distribution across constituent phases, hashin_shtrikman_mp returns candidate theoretical materials, then searches for real materials in the Materials Project database with properties close to the recommended constituents.

Underlying theory

Estimate effective composite properties with the Hashin-Shtrikman bounds

When designing composites, simple volume-weighted linear combinations of constituent material properties do not yield accurate approximations of the resulting effective composite properties. Instead, for laminates, materials designers often bound the resulting composite properties using equations from constitutive elastic theory, such as the Hill-Reuss-Voight-Weiner bounds, where the lower bound is the harmonic mean of the constituent material properties and the upper bound is the arithmetic mean (Brown, 2015). For quasi-isotropic and quasi-homogeneous multi-phase composites with arbitrary phase geometry (a more general case), a better option is to use the Hashin-Shtrikman bounds, which provide even tighter ranges on the resulting effective properties (Hashin & Shtrikman, 1962). Equation 1 summarizes the Hashin-Shtrikman bounds on a generalized effective material property y^* of an n -phase composite. The generalized material properties for the n -phases are ordered from least to greatest where $y_1 \leq y_2 \leq \dots \leq y_n$ with corresponding volume fractions that sum to unity $v_1 + v_2 + \dots + v_n = 1$, and are given by

$$y_1 + \frac{A_1}{1 - \alpha_1 A_1} = y^{*, -} \leq y^* \leq y^{*, +} = y_n + \frac{A_n}{1 - \alpha_n A_n} \quad (1)$$

where

$$\alpha_1 = \frac{1}{3y_1} \quad \text{and} \quad \alpha_n = \frac{1}{3y_n}, \quad (2)$$

and

$$A_1 = \sum_{i=2}^n \frac{v_i}{\frac{1}{y_i - y_1} + \alpha_1} \quad \text{and} \quad A_n = \sum_{i=1}^{n-1} \frac{v_i}{\frac{1}{y_i - y_n} + \alpha_n}. \quad (3)$$

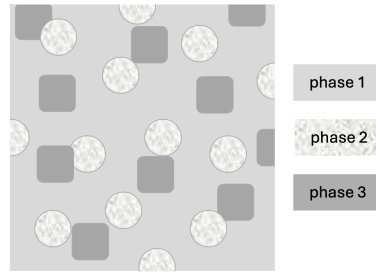


Figure 1: An example of a quasi-isotropic, quasi-homogeneous 3-phase composite.

Equation 4 and Equation 5 summarize the results of the Hashin-Shtrikman derivations on the bounds on effective bulk modulus κ^* and effective shear modulus μ^* , where it is simultaneously required that $\kappa_1 \leq \kappa_2 \leq \dots \leq \kappa_n$ and $\mu_1 \leq \mu_2 \leq \dots \leq \mu_n$:

$$\kappa_1 + \frac{A_1^\kappa}{1 - \alpha_1^\kappa A_1^\kappa} = \kappa^{*, -} \leq \kappa^* \leq \kappa^{*, +} = \kappa_n + \frac{A_n^\kappa}{1 - \alpha_n^\kappa A_n^\kappa} \quad (4)$$

$$\mu_1 + \frac{A_1^\mu}{1 - \alpha_1^\mu A_1^\mu} = \mu^{*, -} \leq \mu^* \leq \mu^{*, +} = \mu_n + \frac{A_n^\mu}{1 - \alpha_n^\mu A_n^\mu} \quad (5)$$

64 with

$$\alpha_1^\kappa = \frac{3}{3\kappa_1 + 4\mu_1} \quad \text{and} \quad \alpha_n^\kappa = \frac{3}{3\kappa_n + 4\mu_n}, \quad (6)$$

65 and

$$\alpha_1^\mu = \frac{3(\kappa_1 + \mu_1)}{5\mu_1(3\kappa_1 + 4\mu_1)} \quad \text{and} \quad \alpha_n^\mu = \frac{3(\kappa_n + \mu_n)}{5\mu_n(3\kappa_n + 4\mu_n)}, \quad (7)$$

66 and

$$A_1^\kappa = \sum_{i=2}^n \frac{v_i}{\frac{1}{\kappa_i - \kappa_1} + \alpha_1} \quad \text{and} \quad A_n^\kappa = \sum_{i=1}^{n-1} \frac{v_i}{\frac{1}{\kappa_i - \kappa_n} + \alpha_n}, \quad (8)$$

67 and

$$A_1^\mu = \sum_{i=2}^n \frac{v_i}{\frac{1}{\kappa_i - \kappa_1} + \alpha_1} \quad \text{and} \quad A_n^\mu = \sum_{i=1}^{n-1} \frac{v_i}{\frac{1}{\mu_i - \mu_n} + \alpha_n}. \quad (9)$$

68 The elastic forms for $\{A_i^\kappa\}$ and $\{A_i^\mu\}$ differ from the general forms $\{A_i\}$ because of their
69 coupling via the Kirchoff-St. Venant constitutive law.

70 Once upper and lower bounds on the effective composite properties have been obtained, what
71 remains is to find a final estimate of the resulting material properties. By the definition of
72 bounds, we can write an expression for the effective property as

$$y^* = \gamma y^{*, -} + (1 - \gamma) y^{*, +}. \quad (10)$$

73 Given experimental data, one could fit γ and extrapolate for a range of volume fractions, but,
74 in the absence of experimental data, the authors select $\gamma = 0.5$. For more information, the
75 reader is referred to (Zohdi & Wriggers, 2008).

76 Quantifying distributed loads with concentration tensors

77 In addition to finding effective properties of potential composites, hashin_shtrikman_mp
78 recommends composites that are less prone to failure under extreme loading. When loads
79 are not efficiently shared between constituents of the composite, stress concentrations, hot
80 spots, and electrical shorts can develop, eventually leading to material failure. By introducing
81 the concept of “concentration tensors”, we can quantify a constituent’s contribution to load
82 response and then use constitutive laws to determine how the composite will respond to loads.

83 For the general case of a constitutive law of the form

$$\text{tensor-valued response} = \text{proportionality tensor} \times \text{tensor-valued load}, \quad (11)$$

84 over the domain Ω , we note that, by the definition of volume fraction, the following holds:

$$\langle \text{tensor-valued load} \rangle_\Omega = \sum_{i=1}^n v_i \langle \text{tensor-valued load} \rangle_{\Omega_i} \quad (12)$$

85 and

$$\langle \text{tensor-valued response} \rangle_\Omega = \sum_{i=1}^n v_i \langle \text{tensor-valued response} \rangle_{\Omega_i}, \quad (13)$$

86 where $\langle \cdot \rangle_\Omega = \frac{1}{|\Omega|} \int_\Omega (\cdot) d\Omega$ is the average of (\cdot) over the domain, v_i is the volume fraction of
87 phase i , and n is the number of phases. From there, we define the concentration tensors for
88 the applied loads and responses for phases $i \in [1, \dots, n]$, respectively, as

$$\langle \text{tensor-valued load} \rangle_{\Omega_i} \equiv C_{i, \text{load}} \langle \text{tensor-valued load} \rangle_\Omega \quad (14)$$

89 and $\langle \text{tensor-valued response} \rangle_{\Omega_i} \equiv C_{i,\text{response}} \langle \text{tensor-valued response} \rangle_{\Omega}. \quad (15)$

It follows from these definitions, and the assumption that the composite is isotropic and homogeneous, that the concentration tensors can be written only in terms of proportionality tensors. The concentration tensors for the applied loads for phases $i \in [2, \dots, n]$ are subsequently given by

94 and for phase 1 as

⁹⁵ The concentration tensors for the responses for phases $i \in [2, \dots, n]$ are given by

96 and for phase 1 as

97 As a concrete example, consider Ohm's law, which relates the applied electric field \mathbf{E} (load) to
98 the resulting current density \mathbf{J} (response) via the electrical conductivity σ_e (proportionality
99 tensor), governing a 3-phase composite. The concentration tensors for current density would
100 be

101 where σ_e^* would be found according to the previous section. The concentration tensors for
102 electric field would be

In the case where the constitutive law governing concentration tensors is the Kirchhoff-St. Venant law, which relates the tensor-valued strain to the tensor-valued stress via the tensor-valued stiffness, we can additionally define scalar-valued concentration factors $C_{i,\kappa}$ and $C_{i,\mu}$, which respectively are the concentration factors for hydrostatic and deviatoric stress. For phases $i \in [2, \dots, n]$ They are defined as

Becker et al. (2025). hashin_shtrikman_mp: a package for the optimal design and discovery of multi-phase composite materials. *Journal of Open Source Software*, *i* VOL? (*i* ISSUE?), *i* PAGE? <https://doi.org/10.xxxxxx/draft>.

108 and

$$C_{i,\mu} = \frac{1}{v_i} \frac{\mu_i}{\mu^*} (\mu^* - \mu_1)(\mu_i - \mu_1)^{-1}, \quad (23)$$

109 where

$$\left\langle \frac{1}{3} \text{tr} \boldsymbol{\sigma} \right\rangle_{\Omega_i} \equiv C_{i,\kappa} \left\langle \frac{1}{3} \text{tr} \boldsymbol{\sigma} \right\rangle_{\Omega} \quad (24)$$

110 and

$$\langle \boldsymbol{\sigma}' \rangle_{\Omega_i} \equiv C_{i,\kappa} \langle \boldsymbol{\sigma}' \rangle_{\Omega}. \quad (25)$$

111 For phase 1, the concentration tensors are defined as

$$C_{1,\kappa} = \frac{1}{v_1} \left(1 - \sum_{i=2}^n v_i C_{i,\kappa} \right) \quad (26)$$

112 and

$$C_{1,\mu} = \frac{1}{v_1} \left(1 - \sum_{i=2}^n v_i C_{i,\mu} \right). \quad (27)$$

113 For more information, the reader is referred to (Zohdi & Wriggers, 2008).

114 Package overview

115 Implementation notes

116 The library has been designed to handle the design of 2- to 10-phase isotropic and homogeneous
 117 composites. All materials in the Materials Project database are available for search through
 118 `hashin_shtrikman_mp`, but it is recommended that users restrict the search bounds for universal
 119 anisotropy to be between 0.5 and 1.5 for results closer to theory. Additionally, at the time of
 120 this writing, because of the assumption that the composite and its constituents are isotropic
 121 and homogeneous, the full tensor forms for the effective properties and concentration tensors
 122 are collapsed to scalar forms. This is simpler computationally and allows the same code to
 123 be used for all properties (aside from bulk and shear moduli, which cannot be decoupled).
 124 For material properties in the Materials Project database with full tensor values available,
 125 `hashin_shtrikman_mp` uses the largest eigenvalue. Figure 2 is a flow chart demonstrating the
 126 most common usage of `hashin_shtrikman_mp`.

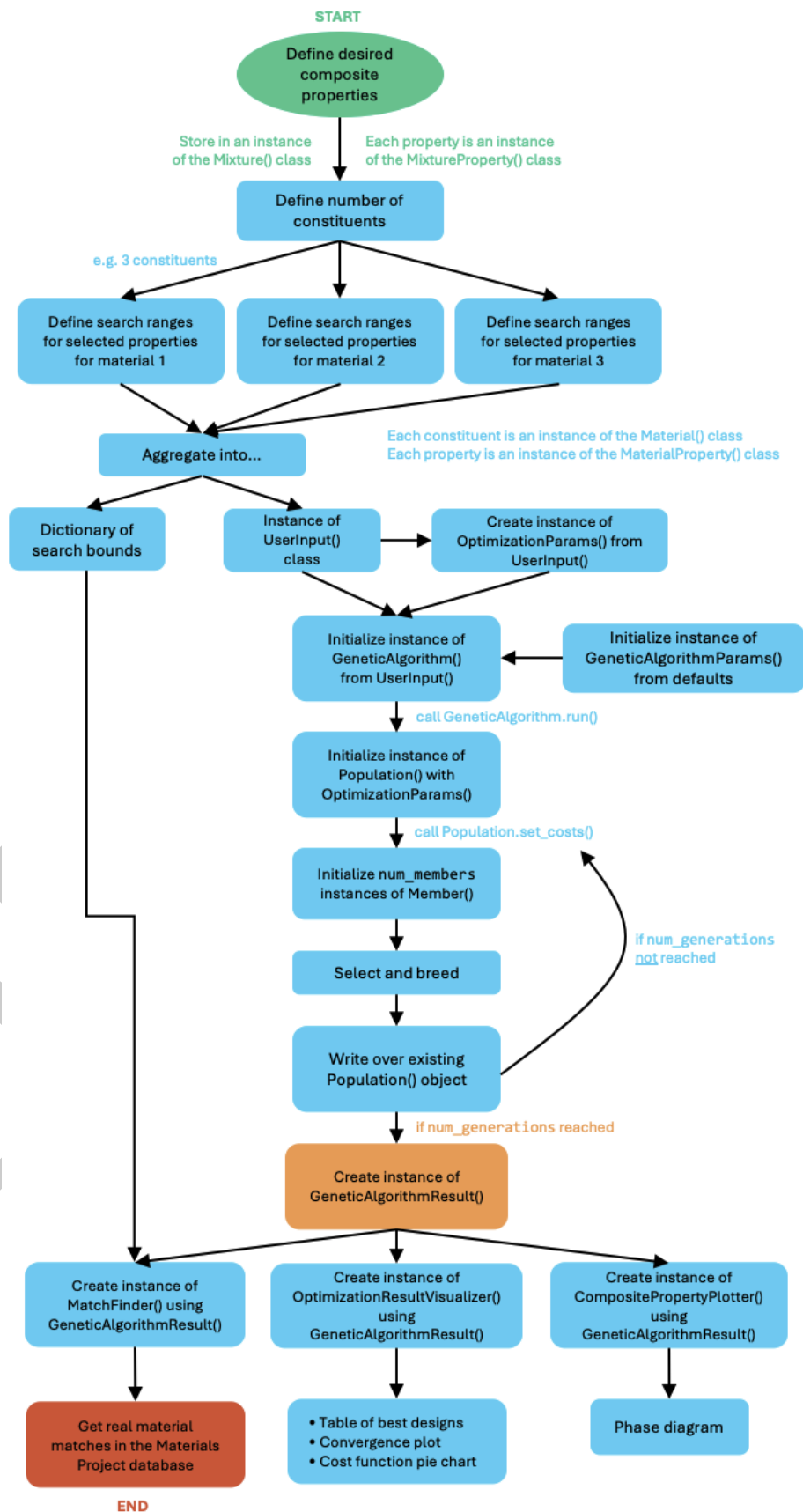


Figure 2: A flow chart demonstrating the most common usage of hashin_shtrikman_mp.

127 Cost function design and optimization with genetic algorithm

128 To find optimal composite mixtures, `hashin_shtrikman_mp` simultaneously seeks composite
129 compositions with effective properties close to the desired properties and seeks to ensure
130 even load sharing among the composite constituent phases. Accordingly, the cost function is
131 constructed in the following way.

132 Each property category selected by a user contributes its own term to the total cost function. At
133 the time of this writing, the possible property categories are elastic, dielectric, carrier-transport,
134 magnetic, and piezoelectric. Combining the individual cost functions to optimize across all
135 design goals simultaneously yields

$$\Pi^{\text{total}} = W_{\text{domains}} [\Pi^{\text{elastic}} + \Pi^{\text{dielectric}} + \Pi^{\text{carrier-transport}} + \Pi^{\text{magnetic}} + \Pi^{\text{piezoelectric}}] \quad (28)$$

136 where W_{domains} normalizes for the number of active property categories. Each property
137 category contribution is composed of two weighted sums: 1) one with terms for absolute error
138 between the effective and desired properties and 2) another for the absolute error between the
139 concentration factors and a tolerance TOL that quantifies “well-distributed” load sharing. That
140 is,

$$\Pi^{\text{general}} = \begin{cases} w_{\text{eff}} \sum_{i=1}^{n_{\text{props}}} \left| \frac{y_i^{*,D} - y_i^*}{y^{*,D}} \right| + \sum_{i=1}^{n_{\text{cfs}}} \hat{w}_{\text{cf}}^i \left| \frac{C_i - \text{TOL}}{\text{TOL}} \right|, & \text{if property category active,} \\ 0, & \text{else,} \end{cases} \quad (29)$$

141 where the superscript D denotes the desired value, n_{props} is the number of properties in that
142 property category, n_{cfs} is the number of concentration factors in that category (typically two \times
143 the number of properties), and C_i is a general scalar-valued concentration factor from section
144 “Quantifying distributed loads with concentration tensors”. Note also that $w_{\text{eff}} = 1/n_{\text{props}}$ and

$$\hat{w}_{\text{cf}}^i = \begin{cases} w_{\text{cf}}, & C_i > \text{TOL}, \\ 0, & \text{otherwise,} \end{cases}$$

145 where $w_{\text{cfs}} = 1/(2n_{\text{props}}n_{\text{materials}})$, except in the elastic case where $w_{\text{cfs}} = 1/n_{\text{props}}n_{\text{materials}}$.

146 As a concrete example, the dielectric contribution to the cost function would take the form

$$\Pi^{\text{dielectric}} = \begin{cases} w_{\text{eff}} \left| \frac{\epsilon^{*,D} - \epsilon^*}{\epsilon_{ij}^{*,D}} \right| + \hat{w}_{\text{cf}}^{i,E} \left| \frac{C_{i,E} - \text{TOL}}{\text{TOL}} \right| + \hat{w}_{\text{cf}}^{i,E_0} \left| \frac{C_{i,E_0} - \text{TOL}}{\text{TOL}} \right|, & \text{if dielectric property category active,} \\ 0, & \text{else,} \end{cases} \quad (30)$$

147 where the constitutive law, in the scalar case, relates applied field E_0 to resulting field E via
148 the dielectric constant ϵ according to $E = \epsilon E_0$ and the same rules for the weights apply as
149 above.

150 With the cost function defined, `hashin_shtrikman_mp` converges to an optimal solution with
151 a genetic algorithm. Each member of a population in the genetic algorithm is composed
152 of candidate material property values. After successive selection and breeding over many
153 generations, the genetic algorithm will converge. The default genetic algorithm parameters are
154 10 parents, 10 children, 200 members per population, and 100 generations, but a user can
155 change them. Given the cost function design, the cost value can be thought of as the fractional
156 error from the desired outcome, plus penalties for “bad” load sharing (should contribute 0 in
157 the case of “good” load sharing). A user can monitor the results of the genetic algorithm with
158 the convergence plot, an example of which is included in Figure 3.

159 The nature of genetic algorithms is to produce several offspring with the same properties and
160 costs after many generations. Thus, hashin_shtrikman_mp presents the user with only the
161 *unique* top performing designs in a table. For the singular lowest-cost performer, users are
162 presented with a breakdown of the cost, as in Figure 4.

163 Visualization and analysis

164 hashin_shtrikman_mp provides visualization tools for the genetic algorithm results and for
165 matches with 2-, 3-, or 4- phases.

166 Figure 3 is a convergence plot showing the value of the genetic algorithm cost function
167 decreasing over generations. The monotonically decreasing staircase nature is characteristic
168 of genetic algorithm convergence, where the best performer may remain the best for several
169 generations and where several genetic strings may converge to the same value (e.g. when
170 the average cost of top ten performers equals the best cost). As the cost function has been
171 designed to represent absolute error from the desired properties, a cost of 1.0 represents 100%
172 error.

173 Figure 4 contains a breakdown of the non-zero cost at the end of optimization for a 3-phase
174 material where the properties of interest were electrical conductivity, thermal conductivity,
175 bulk modulus, shear modulus, and universal anisotropy. We expect the cost function to have
176 31 terms in this case, as there is one effective property term per property and there are two
177 concentration factor terms per property per material, except in the coupled case of bulk and
178 shear moduli, where there are two concentration factors per material instead of the expected
179 four i.e.

- 180 ■ 5 effective properties: one for each of the properties of interest,
- 181 ■ 18 non-modulus concentration factors: one load and one response concentration factor
182 for each of the 3 non-elastic properties (electrical conductivity, thermal conductivity, and
183 universal anisotropy), and for each of the 3 phases, and
- 184 ■ 6 modulus concentration factors: one hydrostatic and one deviatoric concentration factor
185 for each of the 3 phases.

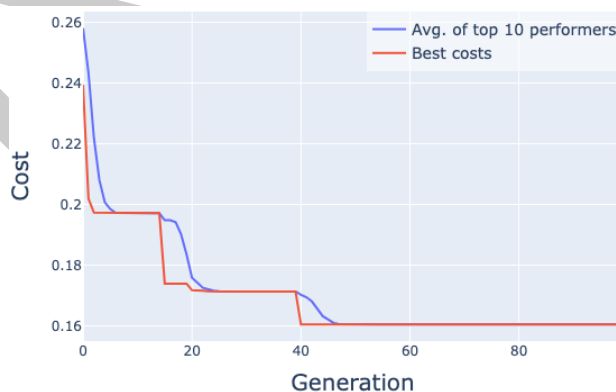


Figure 3: An example of the convergence plot for the genetic algorithm.

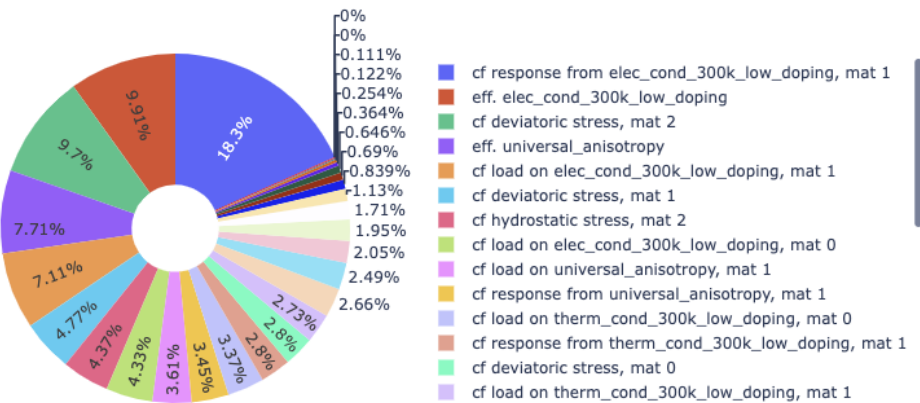


Figure 4: A breakdown of the contributions to the non-zero cost at the end of optimization. Due to the scrollable nature of the legend, only a subset of the 31 entries is visible.

186 Once matches have been identified for a desired composite, along with recommended volume
187 fractions, a user can still explore how varying the volume fractions of the constituents affect
188 the resulting effective properties through interactive phase diagrams. Examples of these phase
189 diagrams are included in Figure 5, Figure 6, and Figure 7.

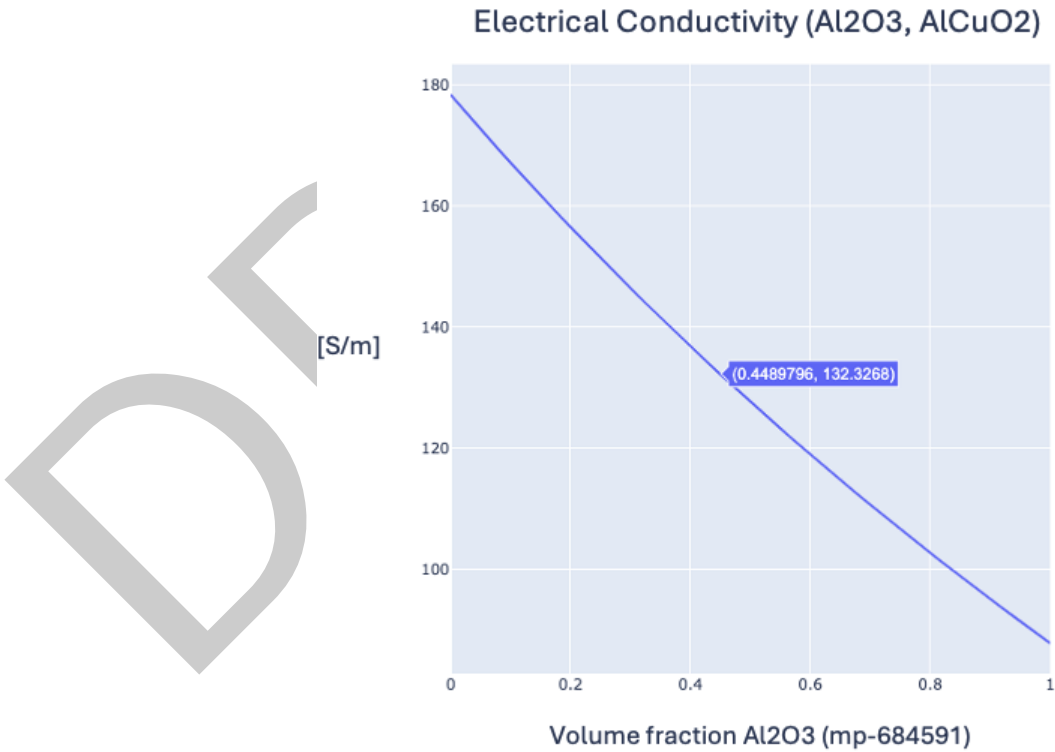


Figure 5: Example phase diagram for a 2-phase mixture of Al_2O_3 and AlCuO_2 . The “mp” numbers are the Materials Project IDs for the materials.

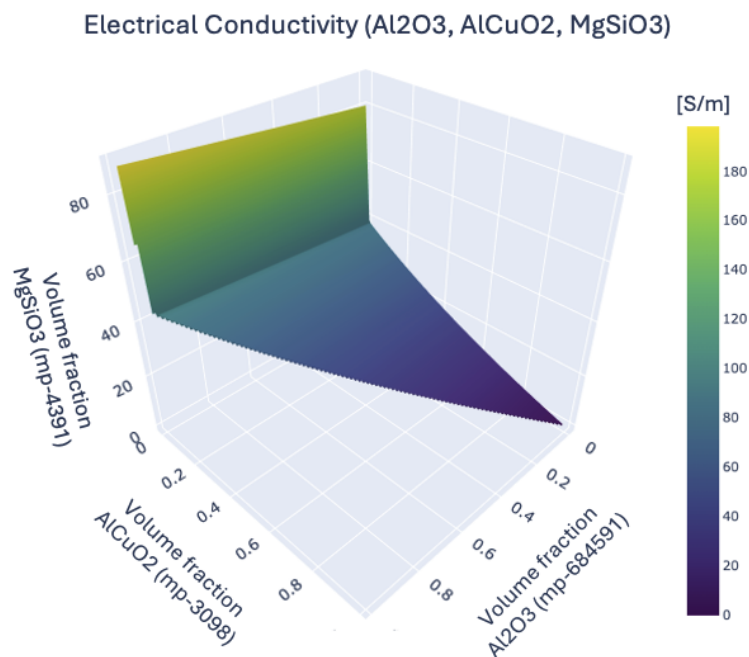


Figure 6: Example phase diagram for a 3-phase mixture of Al₂O₃, AlCuO₂, and MgSiO₃.

Electrical Conductivity (Al₂O₃, AlCuO₂, MgSiO₃, MgAl₂O₄)

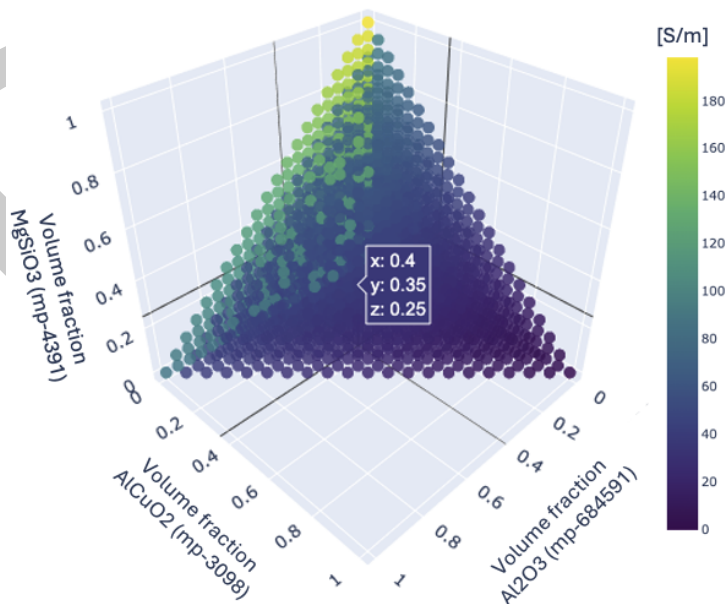


Figure 7: Example phase diagram for a 4-phase mixture of Al₂O₃, AlCuO₂, MgSiO₃ and MgAl₂O₄.

Match-finding

The genetic algorithm returns suggested material properties for each of the phases in the composite and then `hashin_shtrikman_mp` finds real materials in the Materials Project database which are similar, according to some percent error threshold, which the user can control.

Acknowledgments

This work was primarily funded by the Materials Project, which is funded by the U.S. Department of Energy, Office of Science, Office of Basic Energy Sciences, Materials Sciences and Engineering Division, under Contract no. DE-AC02-05-CH11231: Materials Project program KC23MP. The project has been intellectually led by Tarek Zohdi and Kristin Persson. We would also like to thank the software engineering team at the Materials Project – Patrick Huck, Jason Munro, and Ruoxi Yang – for their support.

References

- Brown, J. M. (2015). Determination of hashin-shtrikman bounds on the isotropic effective elastic moduli of polycrystals of any symmetry. *Computers & Geosciences*, 80, 95–99. <https://doi.org/10.1016/j.cageo.2015.03.009>
- Hashin, Z., & Shtrikman, S. (1962). A variational approach to the theory of the effective magnetic permeability of multiphase materials. *Journal of Applied Physics*, 33(10), 3125–3131. <https://doi.org/10.1063/1.1728579>
- Zare, Y., & Rhee, K. Y. (2017). Development of hashin-shtrikman model to determine the roles and properties of interphases in clay/CaCO₃/PP ternary nanocomposite. *Applied Clay Science*, 137, 176–182. <https://doi.org/10.1016/j.clay.2016.12.033>
- Zerhouni, O., Tarantino, M. G., & Danas, K. (2019). Numerically-aided 3D printed random isotropic porous materials approaching the hashin-shtrikman bounds. *Composites Part B: Engineering*, 156, 344–354. <https://doi.org/10.1016/j.compositesb.2018.08.032>
- Zohdi, T. I. (2012). *Electromagnetic properties of multiphase dielectrics: A primer on modeling, theory and computation* (Vol. 64). Springer Science & Business Media. <https://doi.org/10.1007/978-3-642-28427-4>
- Zohdi, T. I., & Wriggers, P. (2008). *Introduction to computational micromechanics*. Springer-Verlag. <https://doi.org/10.1007/11672913>